# Telomerase immortalization upregulates Rab9 expression and restores LDL cholesterol egress from Niemann-Pick C1 late endosomes

**Marc Walter, Joanna P. Davies, and Yiannis A. Ioannou[1]**

Department of Human Genetics, Mount Sinai School of Medicine, New York, NY 10029

**Abstract** **Niemann-Pick C (NPC) disease is a rare recessive lipidosis marked by excessive accumulation of LDL-derived free cholesterol and glycosphingolipids in the late endosomal-lysosomal (E-L) system. Here we report that ectopic expression of human telomerase reverse transcriptase (hTeRT) in human cells leads to an upregulation of the small GTPase Rab9 and its effector p40. Expression of hTeRT in NPC1 cells results in a correction of their cellular phenotype, including clearance of accumulated cholesterol from their E-L system. Specifically, in NPC1-TeRT cells, the transport of cholesterol from the E-L system to the plasma membrane is restored with a concomitant increase in cholesterol esterification. This effect is Rab9-specific since expression of Rab9 in untransformed NPC1 cells also leads to a reversal of their disease phenotype. These effects are also seen in normal TeRT-immortalized cells and it appears that TeRT expression leads to an increase in the transport of molecules, including cholesterol, from the E-L system, and may play a role in increasing cellular proliferation. These results suggest the existence of alternative endogenous therapeutic targets that can be modulated to reverse the NPC1 disease phenotype.**—Walter, M., J. P. Davies, and Y. A. Ioannou. **Telomerase immortalization upregulates Rab9 expression and restores LDL cholesterol egress from Niemann-Pick C1 late endosomes.** ***J. Lipid Res.*** **2003.** 44: **243–253.**

**Supplementary key words** *trans*-Golgi network • endosomal-lysosomal system • human telomerase reverse transcriptase

Niemann-Pick type C (NPC) is a rare autosomal recessive lipidosis characterized by the accumulation of unesterified cholesterol in lysosomes (1, 2). Patients exhibit progressive neurodegeneration and hepatosplenomegaly, which leads to death during early childhood (3). NPC cells accumulate LDL-derived unesterified cholesterol in the endosomal-lysosomal (E-L) system and the *trans*-Golgi network (TGN) (1), and in addition, display delayed cholesterol relocation to and from the plasma membrane (3). The defect of cholesterol exit from the E-L system leads to attenuation in the downregulation of key components that maintain cholesterol homeostasis, such as 3-hydroxy-3-methylglutaryl CoA reductase and the LDL receptor (4).

NPC disease is caused primarily by defects in the *NPC1* gene (5), although about 5% of NPC result from defects in a second gene, *NPC2* (6), that encodes the previously characterized small soluble lysosomal protein, HE1. NPC1 is a membrane glycoprotein that resides primarily in Rab7-positive late endosomes and secondarily in lysosomes and the TGN (7). This distinction is important in view of data suggesting that cholesterol accumulation in $NPC1^{-/-}$ cells occurs primarily in late endosomes (8), which are sorting sites for various cellular components. In support of these observations, NPC1 cells also appear to be defective in the efflux of endocytosed sucrose and in the sorting of the mannose-6 phosphate receptor, suggesting that the retrograde movement of proteins and cargo from late endosomes to the TGN is perturbed (8, 9).

Further characterization of the effects of absent or mutated NPC1 protein suggest that $NPC1^{-/-}$ cells have a generalized block in lipid recycling from late endosomes to the Golgi and plasma membrane (10). Recent studies have implicated NPC1 in the regulation of lipid movement late in the endocytic pathway, presumably from late endosomes (11–13). Studies in Chinese hamster ovary cells have shown that an increase in NPC1 expression leads to a concomitant increase in the transport of LDL-cholesterol (LDL-C) to the plasma membrane (14), lending further support to the idea that NPC1 is involved in subcellular lipid transport. Moreover, expression of human NPC1 in *Escherichia coli* has posited NPC1 as the first mammalian member of an ancient family of prokaryotic pumps that function as multidrug permeases (15).

Detailed studies of NPC1 function in human cells have

*Manuscript received 12 June 2002 and in revised form 24 October 2002.*

*Published, JLR Papers in Press, November 4, 2002.*
*DOI 10.1194/jlr.M200230-JLR200*

Abbreviations: E-L, endosomal-lysosomal; NPC, Niemann-Pick type C; TeRT, telomerase reverse transcriptase; TGN, *trans*-Golgi network.

[1] To whom correspondence should be addressed.
e-mail: yiannis.ioannou@mssm.edu

been hindered by difficulties in growing and maintaining human NPC1 fibroblasts. To alleviate these problems, human fibroblasts can be immortalized by expression of the large T antigen of SV40 virus (16). Recently, expression of human telomerase reverse transcriptase (TeRT) in mammalian cells has been shown to increase their lifespan (17), presumably by preventing the progressive shortening of overall telomere length (18) during each round of DNA replication that leads to replicative senescence (19). It has been proposed that the ability of TeRT-expressing cells to maintain extended telomeres (20) functions not only to preserve genomic stability by preventing chromosome loss, but also to protect against end-to-end chromosome fusion (21).

Although the maintenance of telomere length by TeRT has been extensively characterized (22), cellular changes that may be necessary for maintaining increased cellular proliferation and extended life span have not been identified. We report here that TeRT expression in normal and NPC cells leads to an upregulation of the small GTPase Rab9, which in turn releases the NPC1 cholesterol block. Thus, telomerase expression may promote extended cell proliferation not only by maintaining telomere length, but also by modulating additional intracellular changes, such as Rab9-specific transport from late endosomes to the TGN. These changes may be important in maintaining continued cell proliferation and offer novel targets for modulating both the effects of telomerase and the treatment of NPC disease.

## MATERIALS AND METHODS

### Materials

Dulbecco's modified Eagle's medium (DMEM) and FBS were purchased from Mediatech (Herndon, VA) and HyClone (Logan, Utah), respectively. Filipin (5 mg/ml in DMSO) was from Polysciences Inc., (Warrington, PA). Low-density lipoprotein-deficient serum (LPDS), 2-hydroxypropyl-β-cyclodextrin, and the Protease Inhibitor cocktail for mammalian cells were purchased from Sigma-Aldrich (Milwaukee, WI). L-glutamine, gentamicin, G418, Lipofectamine Plus reagents, and NuPage gels and buffers were from Invitrogen (Carlsbad, CA). [9,10-$^3$H(N)]oleic acid (15 Ci/mmol) and [1,2,6,7-$^3$H(N)]cholesteryl oleate (60 Ci/mmol) were obtained from NEN Life Science Products, (Boston, MA). LDL was obtained from Biomedical Technologies Inc, (Stoughton, MA). The pDON-A1 retroviral vector was from Panvera Corporation (Madison, WI), and the pGRN145 plasmid containing a cDNA encoding human telomerase was a kind gift from Geron Corporation (Menlo Park, CA). The pFB-neo, pMC1neo and pIRES-hr green fluorescent protein (GFP) 1a vectors were from Stratagene (La Jolla, CA), and the PT67 virus-packaging cell line was obtained from Clontech (Palo Alto, CA). Polyclonal anti-NPC1 antibodies were as previously described (15). Polyclonal anti-caveolin, anti-Rab7 and anti-Rab9 antibodies and the anti-SV40 large T antigen monoclonal antibody were from BD Pharmingen (San Diego, CA). HRP-conjugated anti-goat-IgG and anti-rabbit-IgG antibodies were from Santa Cruz Biotechnologies Inc. (Santa Cruz, CA), and the anti-p40 antibody was a generous gift of S. R. Pfeffer (23). The Lumilight Plus substrate was from Roche (Indianapolis, IN), and the TRAPezeXL Telomerase Detection Kit was obtained from Intergen (Purchase, NY).

### Expression vectors

A cDNA encoding the SV40 large T antigen and the SV40 early promoter and enhancer was excised from plasmid pMK16 [which contains a replication origin-defective, full-length copy of the SV40 genome (16)] by digestion with *Bam*HI and *Asp*718. This fragment was ligated into the same restriction sites in pUC19 to generate pUC19-SV(−)T. A DNA cassette encoding the thymidine kinase (TK) promoter, neomycin resistance gene, and TK poly A signals was recovered from plasmid pMC1neo by digestion with *Xho*I and *Sal*I. This fragment was ligated into the *Sal*I site of pUC19-SV(−)T to generate the pTTK-neo vector.

The telomerase expression vector was constructed by inserting a cDNA encoding the human TeRT (20, 24) into the retroviral expression vector pDON-A1, which directs expression of cloned genes from the human CMV promoter. This vector was modified to contain an *Mfe*I restriction site in its polylinker, allowing ligation to the *Eco*RI ends of the telomerase cDNA, which was excised from plasmid pGRN145. The resulting retroviral vector, pDON-TeRT, was lipofected into the packaging cell line PT67, and the packaged amphotrophic virus was collected from the culture medium after 48 h of growth.

The Rab9 retroviral expression vector was generated by cloning the human Rab9 cDNA (25) into the pFB-neo vector (Stratagene). Infectious retrovirus was produced as above using the PT67 cells. The Rab7- and Rab9 GFP-expressing vectors were generated by cloning the respective cDNAs into the pIRES-hrGFP-1a vector (Stratagene). The Rab7 T22N and Rab9 S21N dominant negative mutants were generated using the megaprimer protocol (26). The mutant cDNAs were confirmed by sequencing and cloned into the pIRES-hrGFP 1a vector, as above.

### Cell culture and transfection

The normal fibroblast cell lines (GM00041B and GM05387) and NPC1 fibroblasts (GM03123) (27) were obtained from Coriell Cell Repositories (Camden, NJ). The NPC2 cell line was a kind gift from A. Fensom (28), and the mouse ovarian granulosa NPC1 cell line, ELC, was derived from the *npc$^{nih}$* mouse (29) and was generously provided by Peter Pentchev. Cell lines were maintained in DMEM supplemented with 10% FBS, 2 mM L-glutamine, and 50 μg/ml gentamicin in a humidified incubator at 37°C with 5% $CO_2$.

Exponentially growing cells were transfected with the pTTK-neo plasmid (see above) using Lipofectamine with Plus reagent, according to the manufacturer's recommendations. Clones expressing the SV40 large T antigen were selected in media containing 350 μg/ml G418 for 2 weeks. Individual clones were isolated using cloning rings, expanded, and characterized for SV40 T expression using an anti-SV40 T antigen antibody and immunofluorescence microscopy using a Nikon Eclipse fluorescence microscope equipped with a CCD camera (Nikon, Melville, NY).

Similarly, cells were infected with the pDON-TeRT retrovirus and selected in 350 μg/ml of G418. Positive clones surviving selection were isolated and characterized as described above. All telomerase-immortalized clones exhibited a higher proliferation rate than their untransformed parental lines, as determined by thiazolyl blue (MTT) hydrolysis (data not shown). In addition, telomerase-expressing cell lines have been maintained in culture for >100 population doublings. Telomerase activity was determined using the TRAPezeXL Telomerase Detection Kit. A cell lysate produced from a cell pellet supplied by the manufacturer was used as a positive control, while negative controls were generated by telomerase heat inactivation at 85°C for 10 min, as recommended by the manufacturer. Fluorescence was measured in a Farrand Spectrofluorometer with the excitation/emission parameters set at 495 nm/516 nm.

### Lipid analyses

*Preparation of [$^3$H]oleate substrate.* Sodium oleate, 16.75 mg, was dissolved in methanol and added to [$^3$H]oleate (in ethanol). The mixture was dried under nitrogen, resuspended in 4.4 ml of 14% fatty-acid free BSA in PBS and filter-sterilized.

*Preparation of [$^3$H]cholesteryl oleate-LDL.* Incorporation of [$^3$H]cholesteryl oleate into LDL particles was essentially as described (30). Briefly, glass tubes were coated with potato starch prior to addition of 2 mg LDL and lyophilization. The lipid core of the immobilized LDL particles was extracted using heptane washes and then replaced by adding 62.5 μCi of [$^3$H]cholesteryl oleate, incubating for 10 min at −20°C, slowly drying under nitrogen, and then resuspending in 1 ml 10 mM Tris-HCl, pH 8.4. The reconstituted, labeled LDL was then filtered though a 0.8 μM pore diameter filter and the protein and label recovery determined to ensure that the specific activity 15,000 cpm/nmol was routinely obtained.

*Cholesterol esterification assay.* Esterification assays were essentially as described (31). Briefly, fibroblasts plated at about 30% confluency were grown for 24 h in 3.5 cm dishes with DMEM medium that contained 10% LPDS. Longer incubation periods were not used as the rapidly dividing SV40-transformed cells did not tolerate growth in the absence of LDL for more than 2 to 3 days. On day 2, 1 ml of fresh DMEM containing 10 μl of [$^3$H]oleate substrate (0.76 nmol of [$^3$H]oleate, 125 nmol of unlabeled Na oleate) and 10% of LPDS ± 50 μg/ml LDL was added to the fibroblasts. The cells were incubated for 16 h, harvested by trypsinization, and washed twice in PBS prior to hypoosmotic lysis by freeze-thawing in 150 μl of water.

To determine the quantity of cholesterol oleate formed, 100 μl of cell lysate was mixed with 100 μl of water and 1 ml of chloroform-methanol (2:1, v/v). Lipids were extracted into the lower organic phase and then dried under nitrogen prior to resuspension in 40 μl of chloroform-methanol (2:1, v/v) that contained 30 μg cholesteryl oleate, a marker standard. Half of the sample was applied to a SIL 60 HPTLC plate (E. Merck, Darmstadt, Germany) and the lipids were separated by TLC using hexane-ethylether-glacial acetic acid (90:10:1, v/v/v). The lipids were visualized using iodine vapor and the [$^3$H]cholesteryl oleate was quantified by liquid scintillation counting. Total protein was determined on a 30 μl aliquot of lysate using the fluorescamine assay as described (32). Total oleate uptake was determined using 10 μl lysate and liquid scintillation counting. Esterification of LDL-derived cholesterol was calculated by subtracting the cholesterol oleate values for cells grown in LPDS from those using full FCS medium. All values were obtained in triplicate and normalized to total cell protein.

*Cholesterol efflux assays.* Cholesterol efflux assays were carried out essentially as previously described (33). Cells were grown in medium containing 5% LPDS for 48 h in six-well dishes to 80% confluency as described above. Cells were then incubated in fresh medium containing 5% LPDS, [$^3$H]cholesteryl-oleate LDL (specific activity = $3.8 \times 10^7$ dpm/mg protein), and 20 μg/ml progesterone for 24 h. The cells were then washed three times with LPDS medium and incubated in LPDS medium containing 2% 2-hydroxypropyl-β-cyclodextrin. The cyclodextrin-containing medium was sampled in 0.5 ml aliquots at the indicated times. At the end of the incubation period, the monolayers were washed and lipids were extracted by incubating cells with isopropyl alcohol for 30 min. Protein concentration was determined by extracting the remaining lipid-free cell residue with 0.5 N NaOH. Unesterified and esterified cholesterol levels in the extracted lipids were determined by thin layer chromatography and scintillation counting. The percent of endocytosed cholesterol retained in cells was calculated as follows: [$^3$H]cholesterol retained in cells = [cell-associated [$^3$H]cholesterol/(cell-associated [$^3$H]cholesterol + medium [$^3$H]cholesterol)] · 100.

### Cell lysis and Western blotting

Cell lines were grown in 150 mm culture dishes to 80% confluency. The cell monolayer was washed twice with PBS (pH 7.4) and the cells harvested in PBS containing 2 mM EDTA. The cell pellet was resuspended in ice-cold lysis buffer, 100 mM Na phosphate, 150 mM NaCl, 2 mM EDTA, and 1% (v/v) Igepal (pH 7.5) with protease inhibitor cocktail solution (1 μl/20 mg tissue). The cell suspension was incubated for 20 min on ice and then passed through a 25-gauge needle to shear DNA, followed by centrifugation at 10,000 *g* for 15 min.

For Western blotting, protein samples were resolved using the NuPage gel system and buffers, as recommended by the manufacturer. Briefly, samples containing 20 μg of total protein were denatured by incubation for 10 min at 70°C. The samples were electrophoresed through a 3-8% Tris-Acetate gel (NPC1) in acetate buffer or a 4–12% Bis-Tris gel in MES buffer (caveolin, p40, Rab7, and Rab9) at a constant voltage of 150 V and 200 V, respectively. The proteins were then transferred onto a nitrocellulose membrane using transfer buffer containing 4.08 g/l bicine, 5.23 g/l Bis-Tris, 0.29 g/l EDTA, and 200 ml /l (v/v) methanol at a constant voltage of 30 V for 1 h. After blotting, the nitrocellulose membranes were air dried, washed for 3 × 5 min in TBST buffer (8.8 g/l NaCl, 7.9 g/l Tris, 0.05% (v/v) Tween 20, pH 7.5), and incubated overnight at 4°C in blocking solution [5% (w/v) non-fat dried milk in TBST]. Proteins were detected by chemiluminescence, using an appropriate primary antibody, an HRP-conjugated anti-goat-IgG or anti-rabbit-IgG secondary antibody, and Lumilight Plus substrate solution.

## RESULTS

### Immortalization of human fibroblasts with SV40 large T antigen or TeRT

To further characterize the function of NPC1, various human cells were transfected with vectors expressing either the SV40 large T antigen or hTeRT (17) to generate cell lines with improved growth characteristics. Fibroblasts immortalized with these vectors included human normal (Wt), NPC1, and NPC2 disease cells. As expected, both SV40 T- and hTeRT-transformed cells grew better in culture than their untransformed counterparts. In addition, hTeRT-immortalized cells exhibited an extended life span (>100 population doublings), a phenotype that has been attributed to the maintenance of telomere length by hTeRT expression (17) (**Fig. 1A**). Conversely, SV40 T-transformed cells that have no detectable telomerase activity (Fig. 1A) did not exhibit an extended lifespan and entered "crisis" after a small number of population doublings.

### Telomerase immortalization leads to correction of the NPC1 phenotype

Transformation of cells with the SV40 T antigen has been shown to cause numerous cellular alterations (34), and thus retention of the NPC1 phenotype in the transformed cell lines was investigated. The free cholesterol accumulation in the E-L system of NPC cells can be easily detected using the cholesterol binding polyene macrolide antibiotic filipin (35). Both NPC1 and NPC2 cells exhibited a bright, punctate fluorescence when probed with filipin (Fig. 1B), indicating the typical accumulation of free cholesterol in vesicles of the E-L compartment, whereas Wt fibroblasts exhibit minimal filipin staining as expected (Fig. 1B). Expres-

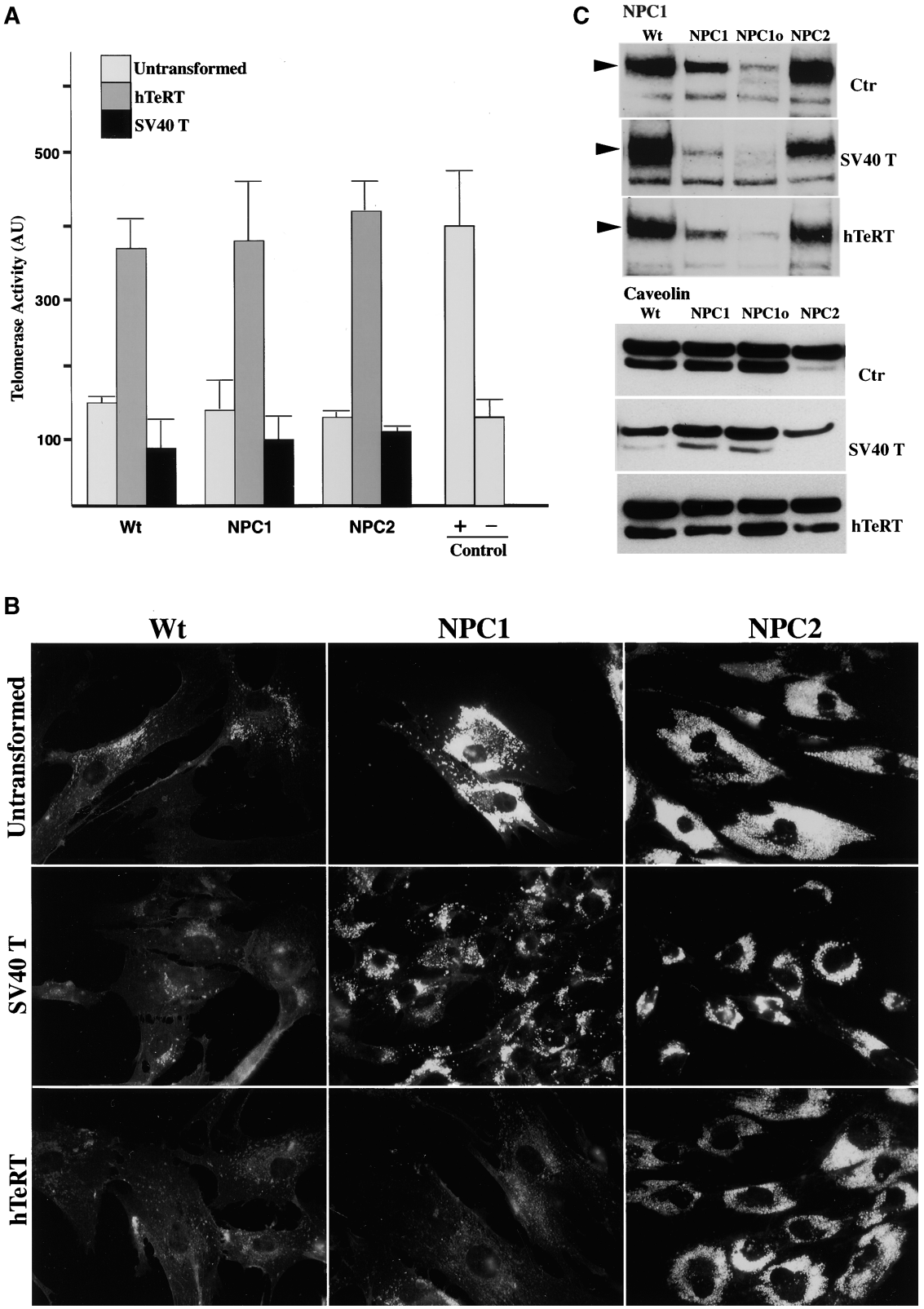


**Fig. 1.** Characterization of wild-type (Wt), human telomerase reverse trascriptase (hTeRT)-, and SV40 T-transformed cell lines. A: Telomerase activity in each cell line was determined using a commercial TRAP assay kit as described in Materials and Methods. Telomerase activity in positive and negative control lysates is denoted by (+) and (−), respectively. Each determination was independently determined at least three times. The average and standard deviation is shown. As expected, telomerase activity (arbitrary units, AU) in untransformed and in SV40 T-transformed cell lines was essentially undetectable, whereas hTeRT-transformed cells exhibit high telomerase activity. B: Wt, Niemann-Pick C (NPC)1, and NPC2 cells stained with filipin to highlight the accumulation of free cholesterol in the E-L system. Wt cells do not exhibit strong filipin staining, whereas NPC1 and NPC2 cells show bright vesicular fluorescence. In contrast, NPC1-TeRT cells lack the strong vesicular staining of the parent cells and appear similar to Wt cells. C: Western-blot analysis of NPC1 expression in the various cell lines. SV40 T- or TeRT-immortalization does not change NPC1 protein expression levels (NPC1 panel; arrows indicate the position of NPC1). The expression of caveolin also remains unchanged in hTeRT-immortalized cell lines (caveolin panel), although its expression is decreased in the SV40 T-immortalized cell lines, as previously described (38).

sion of the SV40 T antigen altered the morphology of all cell lines independent of genotype; however, both NPC1 and NPC2 cells maintained the filipin-positive phenotype of their parental cell lines (Fig. 1B). Similarly, hTeRT expression had no effect on the phenotype of the Wt or NPC2 cells. Surprisingly however, NPC1-TeRT cells no longer accumulated free cholesterol in their E-L system (Fig. 1B). To determine whether this phenotypic change was due to upregulation of a partially active NPC1 protein, Western blot analyses of NPC1 expression were carried out. No increase in NPC1 protein expression was seen in TeRT-immortalized cells (Fig. 1C). Similarly, a second NPC1 cell line that produced negligible amounts of immunoreactive NPC1 protein (NPC1o) also showed no increase in NPC1 protein expression (Fig. 1C). Staining of the NPC1-TeRT cells with filipin revealed that these cells were also corrected and exhibited no cholesterol storage (not shown), suggesting that the clearance of E-L cholesterol in TeRT-immortalized NPC1 cells is independent of NPC1 expression.

Previously, we determined that NPC1 facilitated the efflux of acriflavine from the E-L system (15). However, acriflavine produces high-background fluorescence in mammalian cells due to its inherent ability to bind to DNA. We have determined that the efflux of an acriflavine-related molecule, riboflavine or vitamin B2, from the E-L system is also specifically facilitated by NPC1 and is defective in NPC1 cells (data not shown). Since riboflavine efflux is dependent on NPC1 function, it was predicted that NPC1-TeRT cells would still exhibit a defect if TeRT immortalization did not directly affect NPC1 protein expression and/or function. As expected, Wt cells labeled with riboflavine showed a weak diffuse fluorescence, indicating that this molecule was efficiently transported out of the E-L system (**Fig. 2**). However, both NPC1 and NPC1-TeRT cells retained a bright vesicular

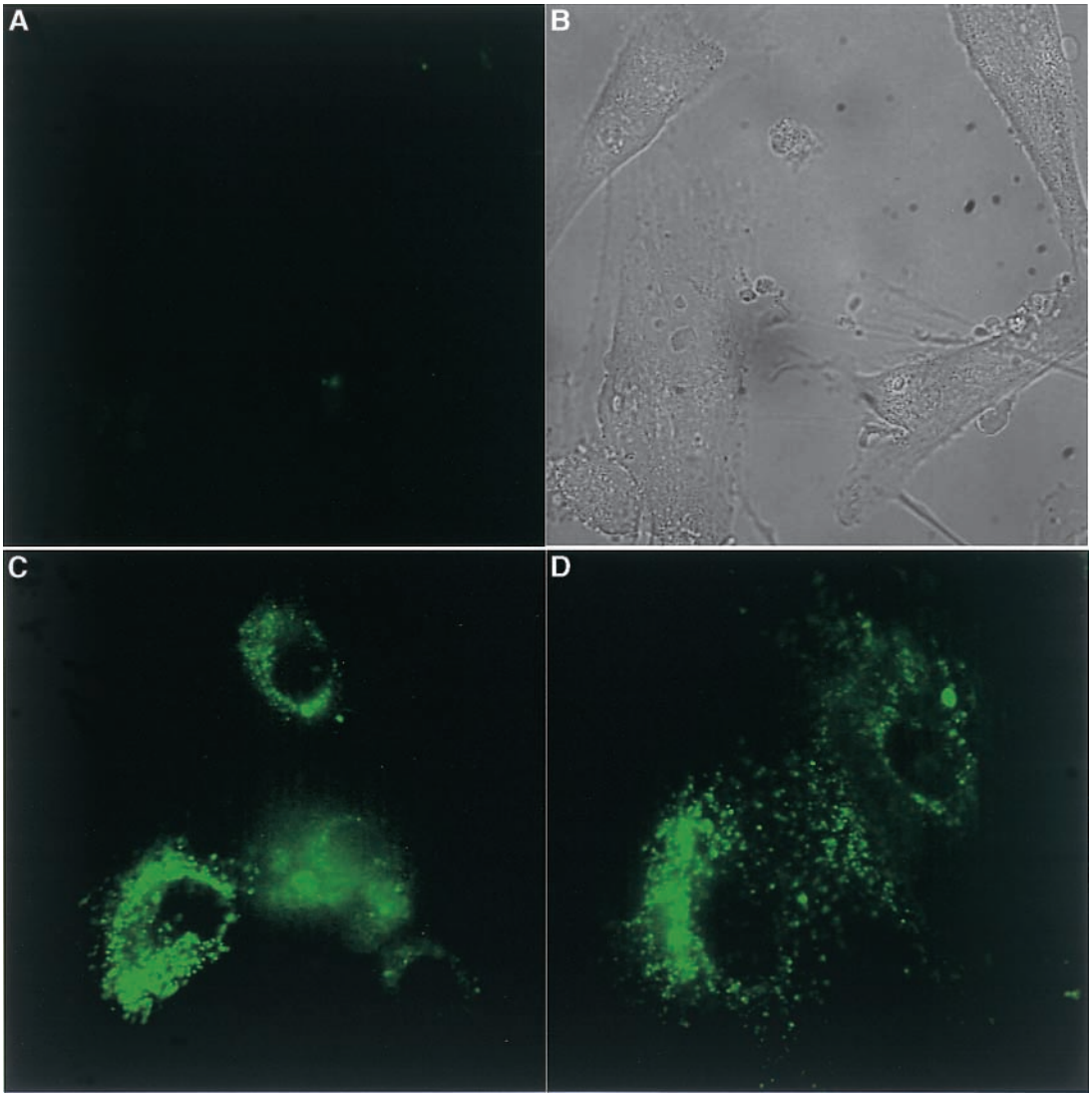


**Fig. 2.** Riboflavine efflux in Wt, NPC1, and NPC1-TeRT cells**.** Cells were plated on glass coverslips, incubated with 100 μg/ml riboflavine for 16 h, and viewed live with a Nikon eclipse microscope using the FITC filter set. In Wt cells, the transport of endocytosed riboflavine, like acriflavine (15), out of the E-L system by NPC1 is indicated by the absence of riboflavine vesicular fluorescence (A; B, phase contrast image of cells shown in A). In contrast, both NPC1 (C) and NPC1-TeRT (D) cells exhibit bright vesicular fluorescence indicating that riboflavine cannot be extruded due to the defective activity of NPC1.

fluorescence, indicating that riboflavine efflux in these cells was still compromised (Fig. 2C, D).

Caveolin has been implicated in the transport of cholesterol from the TGN to the plasma membrane (36). A role for NPC1 in this pathway has also been suggested (2), since NPC1 cells have a block in cholesterol transport from the TGN to the plasma membrane (2, 37). To determine whether correction of the NPC1 phenotype by TeRT involves alterations in caveolin expression, Western blot analysis was performed as above. The SV40 T-transformed cells exhibited a downregulation of caveolin expression that is consistent with previous reports (38). However, no changes in caveolin expression were apparent in the TeRT-immortalized cells (Fig. 1C), indicating that correction of the NPC1 phenotype did not involve changes in caveolin expression.

Following its departure from the E-L system, cholesterol arrives at the plasma membrane where most cellular free cholesterol is maintained (39). To determine whether this pathway is restored in NPC1-TeRT cells, the transport of free cholesterol to the plasma membrane was monitored using 2-hydroxypropyl-β-cyclodextrin (33). As expected, untransformed NPC1 cells exhibited a delayed arrival of free cholesterol at the plasma membrane (33), as shown by the greater amount of cholesterol retained in cells compared with Wt cells (**Fig. 3A**). However, in NPC1-TeRT cells, cholesterol arrived at the plasma membrane at a rate similar to Wt cells (Fig. 3A), suggesting that hTeRT immortalization restored this pathway in NPC1 cells. Next, plasma membrane cholesterol was monitored for its movement to the endoplasmic reticulum (ER) for subsequent esterification by ACAT. Wild-type and NPC1 cells transformed with SV40 T antigen showed an increase in cholesterol esterification (Fig. 3B), which may reflect a direct effect of SV40 T transformation (40) such as alterations in the regulation of the LDL receptor (40). More significantly, NPC1-TeRT cells showed a 3–4-fold increase in cholesterol esterification in comparison to their untransformed counterpart (Fig. 3B), indicating that in these cells, cholesterol can exit the E-L system and be targeted to the ER for esterification. It should be noted however, that this increase in esterification could be partly due to upregulation of ACAT by telomerase.

As discussed above, a direct consequence of the cholesterol efflux block in NPC1 cells is their altered cellular cholesterol homeostasis due to an upregulation of the sterol regulated element (SRE) response (3). To conclusively demonstrate that NPC1 cells are rescued following TeRT expression, we monitored the SRE response of these cells with a vector that drives the expression of GFP under the control of a double SRE motif (41). In this vector system, GFP expression is off or downregulated when cells sense ample cholesterol and is greatly upregulated when cells detect a lack of cholesterol (41). Thus, introduction of this vector in normal cells in the presence of cholesterol would result in very little GFP expression, whereas introduction into NPC cells would result in high GFP expression even in the presence of cholesterol. As expected, introduction of this vector in NPC1 cells resulted in high GFP expression that was not downregulated in the presence of LDL (Fig. 3C; NPC1). Similar to previous results (41), growth of Wt cells in the presence of LDL downregulated GFP expression, whereas LDL depletion caused an increase in GFP expression (Fig. 3C; Wt). Wt-TeRT cells responded similarly to the presence or absence of LDL, although induction of GFP expression in the absence of LDL was less than that in Wt cells (Fig. 3C; Wt-TeRT). Interestingly, NPC1-TeRT cells responded similarly to Wt cells with reduced GFP expression in the presence of LDL (Fig. 3C; NPC1-TeRT), indicating that these cells have bypassed the cholesterol efflux block exhibited by the parental NPC1 cells.

### Telomerase immortalization leads to upregulation of late endosome to TGN transport

Transport of lipids and proteins from the E-L system to the TGN depends on the small GTPases Rab7 and Rab9 (42). Western blot analyses were carried out to determine whether the expression of these proteins was altered in TeRT-immortalized cells. As shown in **Fig. 4**, the expression of Rab7 was unchanged between normal and TeRT-immortalized cells (Fig. 4A), suggesting that Rab7 is not involved in cholesterol clearance from late endosomes, consistent with a recent report (43). However, the expression of Rab9 was increased approximately 6-fold in Wt TeRT-immortalized cells and ~4-fold in NPC1 TeRT-immortalized cells, suggesting that Rab9 may be responsible for the correction of the NPC1 phenotype (Fig. 4A). Further support for Rab9 involvement in cholesterol egress from the E-L system was provided by the fact that expression of p40, a Rab9-interacting protein necessary for endosome-to-TGN transport (23), was also increased in TeRT-immortalized cells (Fig. 4A). Interestingly, p40 was also upregulated in untransformed NPC1 cells, probably in response to the transport block from late endosomes to the TGN. No further increase in p40 expression could be seen in NPC1-TeRT cells, suggesting that expression of p40 in these cells was maximal and no further upregulation could occur. Treatment of Wt and NPC1 cells with progesterone, which inhibits cholesterol egress from the E-L system (44), caused a dramatic upregulation of Rab9 expression (Fig. 4B), indicating that Rab9 and its effector, p40, are upregulated either when transport from the E-L system to TGN is blocked or when cells are immortalized with TeRT. Interestingly, progesterone had no direct effect on p40 expression, since treatment of Wt cells with progesterone did not result in an increase in p40 expression (data not shown).

To confirm the involvement of Rab9 in the release of the cholesterol transport block in NPC1 cells, these cells were transduced with a retroviral vector expressing human Rab9 (25). As expected, expression of Rab9 alone released the transport block in NPC1 cells, allowing cholesterol to be cleared from the E-L system (Fig. 4C). Interestingly, Rab9-positive late endosomes did not contain cholesterol as detected by filipin staining (Fig. 4C), lending further support to the notion that upregulation of Rab9 expression by TeRT-immortalization can bypass the requirement for the NPC1 protein in late endosome-to-TGN transport.

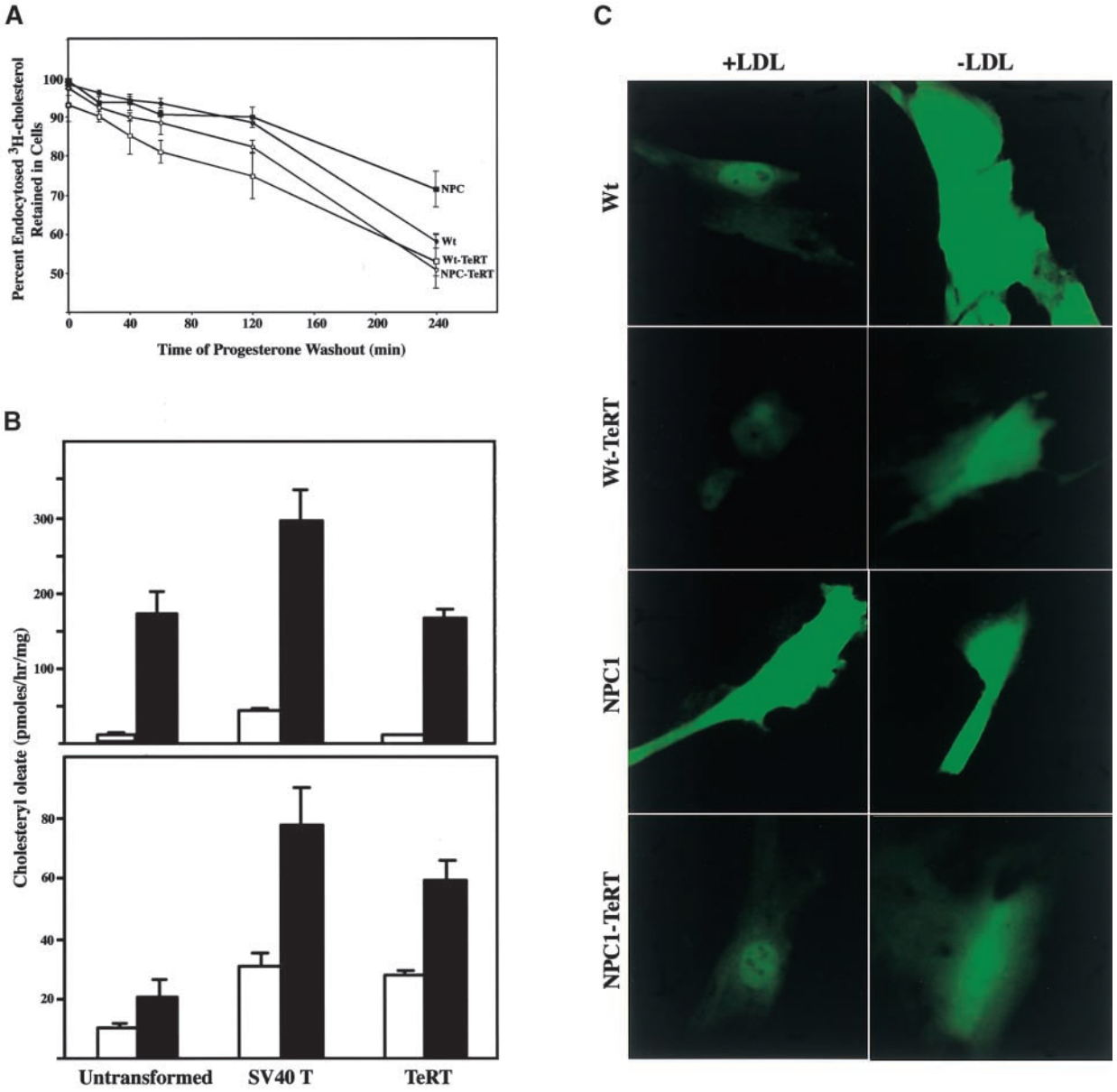


**Fig. 3.** Cholesterol transport to the plasma membrane and endoplasmic reticulum. A: Cholesterol transport to the plasma membrane was measured by labeling cells with LDL-containing [$^3$H]cholesteryl-oleate as described in Materials and Methods. Free cholesterol remaining in cells was determined as detailed in Materials and Methods. Values represent the mean ± SD of triplicate wells. In NPC cells, cholesterol exhibits a delayed transport to the plasma membrane as indicated by its retention in cells. In NPC-TeRT cells however, cholesterol arrives at the plasma membrane similar to Wt, and Wt-TeRT cells, as indicated by its decreased cellular retention. B: Esterification assays were performed to determine whether cholesterol in NPC1-TeRT cells can reach the endoplasmic reticulum for esterification. SV40 T immortalization causes an increase in esterification in both cell lines. TeRT-immortalization has no effect on esterification in Wt cells (top panel). However, NPC1-TeRT cells show a 3–4-fold increase in esterification (bottom panel). Open bars indicate basal esterification in the absence of LDL and closed bars indicate esterification in the presence of LDL. C: Restoration of the sterol-regulated element (SRE) response in NPC1-TeRT cells. Cells were transfected with a plasmid expressing green fluorescent protein (GFP) under the control of an SRE promoter. Growth of Wt or Wt-TeRT cells in the absence of LDL for 24 h causes an upregulation of GFP expression as expected (Wt, Wt-TeRT; −LDL). Also as expected, NPC1 cells are unable to down-regulate the SRE response in the same time period and therefore GFP is upregulated in cells grown in the presence or in the absence of LDL (NPC1; +LDL). This aberrant SRE regulation is corrected in NPC1-TeRT cells (NPC1-TeRT; +LDL). The results shown are representative of a number of different cells in each experiment scored (n = 20).

To further confirm these results, vectors were constructed that could express Rab9 in a bicistronic manner with GFP under the control of the strong cytomegalovirus promoter/enhancer. Thus, Rab9-expressing cells could be readily identified by their GFP-positive phenotype. Vectors for Rab7 and the Rab7 and Rab9 dominant negative mutants, T22N and S21N, respectively, were also constructed using this system. Since transfection of human fibroblasts with plasmid DNA is very inefficient, the mouse NPC1 cell line ELC (45) was used for subsequent analyses. Furthermore, it was noted that human NPC1 cells show heterogeneous filipin phenotypes following growth in LPDS,

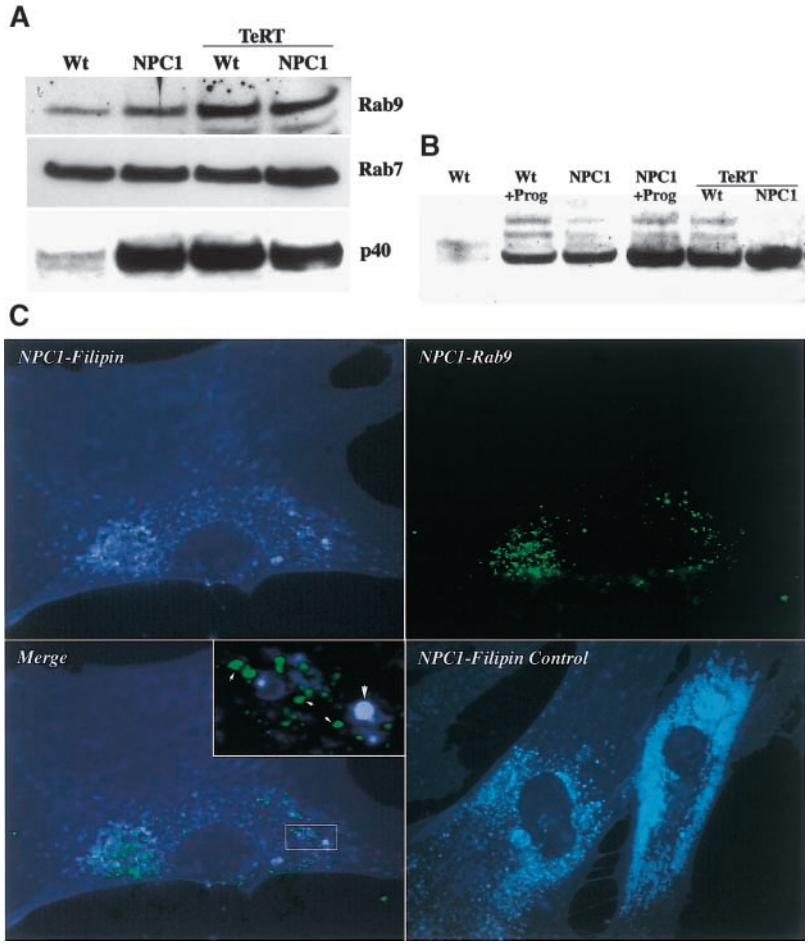


**Fig. 4.** Analyses of Rab GTPase expression. A: Western blot analyses of Rab9, Rab7, and p40 expression in untransformed and TeRT-transformed cells. Rab9 is upregulated ~6-fold in TeRT-immortalized cells, whereas Rab7 is unchanged. Expression of p40 is higher both in TeRT-immortalized and NPC1 cells compared with Wt cells. B: Western blot analysis of Rab9 expression in normal, TeRT-immortalized, and progesterone-treated normal cells. Progesterone treatment (10 μg/ml for 24 h) causes an upregulation of Rab9 expression similar to the expression seen in TeRT-immortalized cells. C: NPC1 cells transduced with a retroviral vector expressing human Rab9 show a clearance of cholesterol storage in NPC1 endosomes (NPC1-Filipin) compared with untransduced NPC1 cells (NPC1-Filipin Control). Of note, Rab9-positive endosomes (NPC1-Rab9) are completely clear of cholesterol (Merge; inset).

with some cells displaying decreased filipin fluorescence. Thus, the mouse cells, which do not exhibit this phenotype (data not shown) can more accurately reflect the effects of Rab9 and Rab7 expression on their filipin-positive phenotype. As shown in **Fig. 5B**, expression of Rab9 in these cells completely cleared the filipin-positive material. Of note, clearance of filipin material was related to the level of Rab9 expression (Fig. 5B). For example, cells that expressed high levels of GFP (which correlates with the levels of Rab9, since the two genes are linked) showed a complete clearance of filipin-positive material (Fig. 5B, large arrows) compared with cells expressing lower levels of GFP, which still displayed some filipin-positive material (Fig. 5B, small arrows). Expression of Rab7 in these cells did not result in the clearance of filipin material (Fig. 5C), further suggesting that, since the expression of Rab7 was not increased in telomerase-expressing cells, Rab7 is not involved in the correction of the NPC1 phenotype following telomerase immortalization. As expected, expression of the Rab9 dominant negative mutant S21N had no effect on the filipin-positive material in these NPC1 cells (Fig. 5D). Interestingly, expression of the Rab7 dominant negative mutant T22N resulted in a high degree of apoptotic cell death (Fig. 5E). In fact, greater than 70% of cells positive for GFP exhibited the multi-fragmented cellular phenotype seen in Fig. 5E ($n > 20$).

## DISCUSSION

The results described here suggest that telomerase immortalization of human cells affects the function of the E-L system and in particular the efflux of cholesterol from this system, independent of the NPC1 protein. Such changes may be necessary to maintain cells in a continued proliferative state (46). In fact, a recent study has provided evidence for a correlation between cholesterol content and cell cycle progression (47). Inhibition of choles-

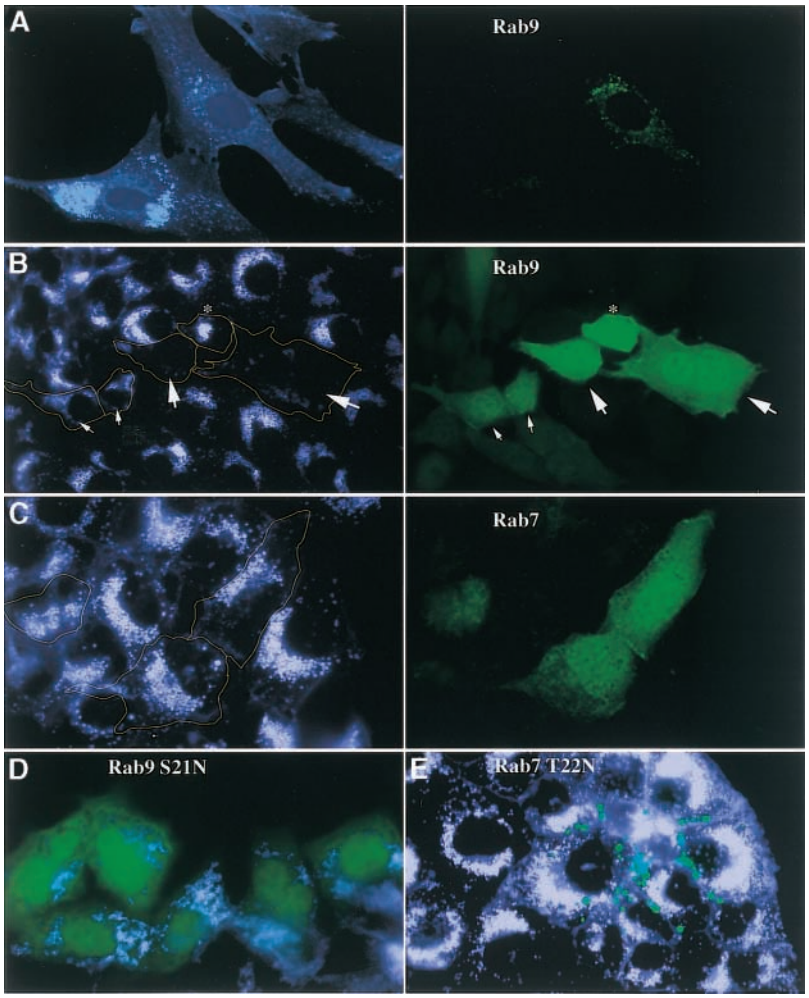


**Fig. 5.** Expression of Rab7 and Rab9 in NPC1 cells. A: As a control, human NPC1 fibroblasts were infected with a Rab9-expressing retrovirus as described in Fig. 4C. Three days postinfection, cells were stained with filipin (left panel) and an anti-Rab9 antibody (right panel). A Rab9-positive cell is completely devoid of filipin-positive material, whereas a neighboring Rab9-negative cell exhibits bright, vesicular filipin staining. B: Mouse NPC1 cells were transfected with a plasmid expressing a bicistronic mRNA for Rab9 and GFP. Thus, the levels of GFP directly reflect the levels of Rab9 expression, since both proteins are translated from a single mRNA. Similar to the results of Rab9 expression in human NPC1 cells (A), expression of Rab9 in mouse NPC1 cells resulted in correction of their filipin-positive phenotype. Notably, the level of correction is directly related to the level of expression, as shown for those with high (large arrows) and low (small arrows) expression. The star denotes a dying cell. C: Expression of Rab7 in a similar manner, as described for Rab9 (B), did not result in any filipin-corrected cells. D: The Rab9 mutant S21N was also unable to correct NPC1 cells. E: Similarly, expression of the Rab7 mutant T22N did not yield any NPC1-corrected cells. However, most cells expressing Rab7 T22N were in the process of undergoing apoptosis.

terol biosynthesis with low concentrations of lovastatin blocked cell proliferation, with cells accumulating in G2. When LDL-C was added to these cells, cell cycle progression was resumed (47). In NPC1 disease, cells are unable to metabolize LDL-derived cholesterol due to its accumulation in the late E-L system. Currently, there is no evidence to suggest that a lack of LDL-derived cholesterol has any impact on cell cycle progression in NPC1 cells other than that NPC1 cells grow very slowly in culture and soon reach a state of replicative senescence. However, NPC1 fibroblasts transformed by hTeRT exhibit an increased life span and grow as rapidly as normal cells in culture.

Thus, it may be important for actively proliferating cells to increase the rate by which they obtain LDL-derived cholesterol. This access could be accomplished by either upregulating late endosome cholesterol efflux via the expression of NPC1 or upregulating cholesterol transport from late endosomes to the TGN. The data presented here suggest that the two mechanisms are independent, since transport of cholesterol from late endosomes to the TGN occurs in the absence of NPC1 and involves the upregulation of the small GTPase Rab9 and its effector, p40. Also, since both Wt and NPC cells upregulate Rab9 expression following TeRT immortalization, it appears that the preferred mechanism is the upregulation of late en-

dosome-to-TGN transport. Such an increase in transport would also allow cells to transport factors other than cholesterol from the E-L system, such as proteins, protein receptors, and other lipids.

Interestingly, Rab7, another small GTPase involved in late endosome transport, was not upregulated by telomerase. A recent report clearly demonstrates that the function of Rab7 may be to direct vesicle movement toward the minus end of microtubules (43, 48) and toward lysosomes. This function would be consistent with a lack of Rab7 upregulation by telomerase, since it would not offer any advantage for late endosome-to-TGN transport. During the preparation of this manuscript, another report appeared confirming that Rab9 expression in NPC1 cells corrects the NPC1 phenotype (49). However, in contrast to our results, expression of Rab7 was also shown to correct the NPC1 phenotype. The reasons for these Rab7 conflicting results are not clear, but may partially stem from differences in expression constructs or differences in cell lines used for these studies and perhaps differences in the growth conditions of NPC1 cells prior to and during the transfection/correction experiments. Further work is necessary to establish the exact role of Rab7 in this transport pathway. The Rab7 T22N studies are intriguing and suggest that a deficiency of Rab7 cannot be tolerated, leading to programmed cell death of NPC1 cells. Thus, Rab7 may provide an essential function for the survival of NPC1 cells.

These studies have identified a new candidate for intervention in NPC1 disease and provide an alternative to correcting the defect of the NPC1 protein. Rab9 is a small, well-characterized protein and it may be simpler to modulate its activity to treat NPC1 disease than to rely on approaches that involve the manipulation of the poorly characterized, large membrane glycoprotein NPC1. Furthermore, these immortalized cells lines and their isogenic untransformed counterparts offer an excellent system to further characterize the mechanism of lipid efflux from the E-L system and the effects of TeRT immortalization on subcellular lipid transport. Further characterization of these cells should reveal new targets for modulating telomerase-dependent changes in cells, such as those of malignant tumors (50), with abnormally upregulated telomerase expression.

This work was supported by National Institutes of Health Grant R01 DK-54736, a grant from the March of Dimes Foundation, and the Ara Parseghian Medical Research Foundation.

## REFERENCES


1. Vanier, M. T., C. Rodriguez-Lafrasse, R. Rousson, N. Gazzah, M-C. Juge, P. G. Pentchev, A. Revol, and P. Louisot. 1991. Type C Niemann-Pick disease: spectrum of phenotypic variation in disruption of intracellular LDL-drerived cholesterol processing. *Biochim. Biophys. Acta.* **1096:** 328–337.
2. Pentchev, P. G., R. O. Brady, E. J. Blanchette-Mackie, M. T. Vanier, E. D. Carstea, C. C. Parker, E. Goldin, and C. F. Roff. 1994. The Niemann-Pick C lesion and its relationship to the intracellular distribution and utilization of LDL cholesterol. *Biochim. Biophys. Acta.* **1225:** 235–243.
3. Patterson, M. C., M. T. Vanier, M. C. Suzuki, J. A. Morris, E. Carstea, E. B. Neufeld, E. J. Blanchette-Mackie, and P. G. Pentchev. 2001. Niemann-Pick Disease Type C: a lipid trafficking disorder. *In* The Metabolic and Molecular Bases of Inherited Disease, vol. III. C. R. Scriver, W. S. Sly, and D. Valle, editors. McGraw-Hill, New York. 3611–3633.
4. Pentchev, P. G., H. S. Kruth, M. E. Comly, J. D. Butler, M. T. Vanier, D. A. Wenger, and S. Patel. 1986. Type C Niemann-Pick disease: a parallel loss of regulatory responses in both the uptake and esterification of low-density lipoprotein-derived cholesterol in cultured fibroblasts. *J. Biol. Chem.* **261:** 16775–16780.
5. Carstea, E. D., J. A. Morris, K. G. Coleman, S. K. Loftus, D. Zhang, C. Cummings, J. Gu, M. A. Rosenfeld, W. J. Pavan, D. B. Krizman, J. Nagle, M. H. Polymeropoulos, S. L. Sturley, Y. A. Ioannou, M. E. Higgins, M. Comly, A. Cooney, A. Brown, C. R. Kaneski, E. J. Blanchette-Mackie, N. K. Dwyer, E. B. Neufeld, T. Y. Chang, L. Liscum, J. F. Strauss III, K. Ohno, M. Zeigler, R. Carmi, J. Sokol, D. Markie, R. R. O'Neill, O. P. van Diggelen, M. Elleter, M. C. Patterson, R. O. Brady, M. T. Vaniev, P. G. Pentchev, and D. A. Tagle. 1997. Niemann-Pick C1 disease gene: homology to mediators of cholesterol homeostasis. *Science.* **277:** 228–231.
6. Naureckiene, S., D. E. Sleat, H. Lackland, A. Fensom, M. T. Vanier, R. Wattiaux, M. Jadot, and P. Lobel. 2000. Identification of HE1 as the second gene of Niemann-Pick C disease. *Science.* **290:** 2298–2301.
7. Higgins, M. E., J. P. Davies, F. W. Chen, and Y. A. Ioannou. 1999. Niemann-Pick C1 is a late endosome-resident protein that transiently associates with lysosomes and the trans-Golgi network. *Mol. Genet. Metab.* **68:** 1–13.
8. Kobayashi, T., M-H. Beuchat, M. Lindsay, S. Frias, R. D. Palmiter, H. Sakuraba, R. G. Parton, and J. Gruenberg. 1999. Late endosomal membranes rich in lysobiphosphatidic acid regulate cholesterol transport. *Nat. Cell Biol.* **1:** 113–118.
9. Neufeld, E. B., M. Wastney, S. Patel, S. Suresh, A. M. Cooney, N. K. Dwyer, C. F. Roff, K. Ohno, J. A. Morris, E. D. Carstea, J. P. Incardona, J. F. Strauss 3rd, M. T. Vanier, M. C. Patterson, R. O. Brady, P. G. Pentchev, and E. J. Blanchette-Mackie. 1999. The Niemann-Pick C1 protein resides in a vesicular compartment linked to retrograde transport of multiple lysosomal cargo. *J. Biol. Chem.* **274:** 9627–9635.
10. Puri, V., R. Watanabe, M. Dominguez, X. Sun, C. L. Wheatley, D. L. Marks, and R. E. Pagano. 1999. Cholesterol modulates membrane traffic along the endocytic pathway in sphingolipid-storage diseases. *Nat. Cell Biol.* **1:** 386–388.
11. Ko, D. C., M. D. Gordon, J. Y. Jin, and M. P. Scott. 2001. Dynamic movements of organelles containing niemann-pick c1 protein: npc1 involvement in late endocytic events. *Mol. Biol. Cell.* **12:** 601–614.
12. Zhang, M., N. K. Dwyer, D. C. Love, A. Cooney, M. Comly, E. Neufeld, P. G. Pentchev, E. J. Blanchette-Mackie, and J. A. Hanover. 2001. Cessation of rapid late endosomal tubulovesicular trafficking in Niemann-Pick type C1 disease. *Proc. Natl. Acad. Sci. USA.* **98:** 4466–4471.
13. Zhang, M., N. K. Dwyer, E. B. Neufeld, D. C. Love, A. Cooney, M. Comly, S. Patel, H. Watari, J. F. Strauss 3rd, P. G. Pentchev, J. A. Hanover, and E. J. Blanchette-Mackie. 2001. Sterol-modulated glycolipid sorting occurs in Niemann-Pick C1 late endosomes. *J. Biol. Chem.* **276:** 3417–3425.
14. Millard, E. E., K. Srivastava, L. M. Traub, J. E. Schaffer, and D. S. Ory. 2000. Niemann-pick type C1 (NPC1) overexpression alters cellular cholesterol homeostasis. *J. Biol. Chem.* **275:** 38445–38451.
15. Davies, J. P., F. W. Chen, and Y. A. Ioannou. 2000. Transmembrane molecular pump activity of Niemann-Pick C1 protein. *Science.* **290:** 2295–2298.
16. Neufeld, D. S., S. Ripley, A. Henderson, and H. L. Ozer. 1987. Immortalization of human fibroblasts transformed by origin-defective simian virus 40. *Mol. Cell. Biol.* **7:** 2794–2802.
17. Bodnar, A. G., M. Oulellette, M. Frolkis, S. E. Holt, C-P. Chiu, M. Morin, C. B. Harley, J. W. Shay, S. Lichtsteiner, and W. E. Wright. 1998. Extension of life-span by introduction of telomerase into normal human cells. *Science.* **279:** 349–352.
18. Harley, C. B., A. B. Futcher, and C. W. Greider. 1990. Telomeres shorten during ageing of fibroblasts. *Nature.* **345:** 458–460.
19. Allsopp, R. C., H. Vaziri, C. Patterson, S. Goldstein, E. V. Younglai, A. B. Futcher, C. W. Greider, and C. B. Harley. 1992. Telomere

lenght predicts replicative capacity of human fibroblasts. *Proc. Natl. Acad. Sci.* **89:** 10114–10118.
20. de Lange, T., and R. A. DePinho. 1999. Unlimited mileage from telomerase? *Science.* **283:** 947–949.
21. Bryan, T. M., and T. R. Cech. 1999. Telomerase and the maintenance of chromosome ends. *Curr. Opin. Cell Biol.* **11:** 318–324.
22. Stewart, S. A., and R. A. Weinberg. 2002. Senescence: does it all happen at the ends? *Oncogene.* **21:** 627–630.
23. Diaz, E., F. Schimmoller, and S. R. Pfeffer. 1997. A novel Rab9 effector required for endosome-to-TGN transport. *J. Cell Biol.* **138:** 283–290.
24. Zhu, J., H. Wang, J. M. Bishop, and E. H. Blackburn. 1999. Telomerase extends the lifespan of virus-transformed human cells without net telomere lengthening. *Proc. Natl. Acad. Sci. USA.* **96:** 3723–3728.
25. Davies, J. P., P. D. Cotter, and Y. A. Ioannou. 1997. Cloning and mapping of human Rab7 and Rab9 cDNA sequences and identification of a Rab9 pseudogene. *Genomics.* **41:** 131–134.
26. Sarkar, G., and S. S. Sommer. 1990. The "megaprimer" method of site-directed mutagenesis. *Biotechniques.* **8:** 404–407.
27. Yamamoto, T., E. Nanba, H. Ninomiya, K. Higaki, M. Taniguchi, H. Zhang, S. Akaboshi, Y. Watanabe, T. Takeshima, K. Inui, S. Okada, A. Tanaka, N. Sakuragawa, G. Millat, M. T. Vanier, J. A. Morris, P. G. Pentchev, and K. Ohno. 1999. NPC1 gene mutations in Japanese patients with Niemann-Pick disease type C. *Hum. Genet.* **105:** 10–16.
28. Steinberg, S. J., D. Mondal, and A. H. Fensom. 1996. Co-cultivation of Niemann-Pick disease type C fibroblasts belonging to complementation groups alpha and beta stimulates LDL-derived cholesterol esterification. *J. Inherit. Metab. Dis.* **19:** 769–774.
29. Loftus, S. K., J. A. Morris, E. D. Carstea, J. Z. Gu, C. Cummings, A. Brown, J. Ellison, K. Ohno, M. A. Rosenfeld, D. A. Tagle, P. G. Pentchev, and W. J. Pavan. 1997. Murine model of Niemann-Pick C disease: mutation in a cholesterol homeostasis gene. [see comments] *Science.* **277:** 232–235.
30. Krieger, M., M. S. Brown, J. R. Faust, and J. L. Goldstein. 1978. Replacement of endogenous cholesteryl esters of low density lipoprotein with exogenous cholesteryl linoleate. Reconstitution of a biologically active lipoprotein particle. *J. Biol. Chem.* **253:** 4093–4101.
31. Goldstein, J. L., S. K. Basu, and M. S. Brown. 1983. Receptor-mediated endocytosis of low-density lipoprotein in cultured cells. *Methods Enzymol.* **98:** 241–260.
32. Ioannou, Y. A., K. M. Zeidner, R. E. Gordon, and R. J. Desnick. 2001. Fabry disease: preclinical studies demonstrate the effectiveness of alpha-galactosidase A replacement in enzyme-deficient mice. *Am. J. Hum. Genet.* **68:** 14–25.
33. Neufeld, E. B., A. M. Cooney, J. Pitha, E. A. Dawidowicz, N. K. Dwyer, P. G. Pentchev, and E. J. Blanchette-Mackie. 1996. Intracellular trafficking of cholesterol monitored with a cyclodextrin. *J. Biol. Chem.* **271:** 21604–21613.
34. Pardinas, J., Z. Pang, J. Houghton, V. Palejwala, R. J. Donnelly, K. Hubbard, M. B. Small, and H. L. Ozer. 1997. Differential gene expression in SV40-mediated immortalization of human fibroblasts. *J. Cell. Physiol.* **171:** 325–335.
35. Bolard, J. 1986. How do the polyene macrolide antibiotics affect the cellular membrane properties? *Biochim. Biophys. Acta.* **864:** 257–304.
36. Conrad, P. A., E. J. Smart, Y. S. Ying, R. G. Anderson, and G. S. Bloom. 1995. Caveolin cycles between plasma membrane caveolae and the Golgi complex by microtubule-dependent and microtubule-independent steps. *J. Cell Biol.* **131:** 1421–1433.
37. Garver, W. S., K. Krishnan, J. R. Gallagos, M. Michikawa, G. A. Francis, and R. A. Heidenreich. 2002. Niemann-Pick C1 protein regulates cholesterol transport to the trans-Golgi network and plasma membrane caveolae. *J. Lipid Res.* **43:** 579–589.
38. Koleske, A. J., D. Baltimore, and M. P. Lisanti. 1995. Reduction of caveolin and caveolae in oncogenically tranformed cells. *Proc. Natl. Acad. Sci. USA.* **92:** 1381–1385.
39. Lange, Y., J. Ye, and T. L. Steck. 1998. Circulation of cholesterol between lysosomes and the plasma membrane. *J. Biol. Chem.* **273:** 18915–18922.
40. Chen, J. K., L. Li, and D. B. McClure. 1988. Altered low density lipoprotein receptor regulation is associated with cholesteryl ester accumulation in Simian virus 40 transformed rodent fibroblast cell lines. *In Vitro Cell. Dev. Biol.* **24:** 353–358.
41. Higgins, M. E., and Y. A. Ioannou. 2001. Apoptosis-induced release of mature sterol regulatory element-binding proteins activates sterol-responsive genes. *J. Lipid Res.* **42:** 1939–1946.
42. Lombardi, D., T. Soldati, M. A. Riederer, Y. Goda, M. Zerial, and S. R. Pfeffer. 1993. Rab9 functions in transport between late endosomes and the trans Golgi network. *EMBO J.* **12:** 677–682.
43. Lebrand, C., M. Corti, H. Goodson, P. Cosson, V. Cavalli, N. Mayran, J. Faure, and J. Gruenberg. 2002. Late endosome motility depends on lipids via the small GTPase Rab7. *EMBO J.* **21:** 1289–1300.
44. Butler, J. D., J. Blanchette-Mackie, E. Goldin, R. R. O'Neill, G. Carstea, C. F. Roff, M. C. Patterson, S. Patel, M. E. Comly, A. Cooney, M. T. Vanier, R. O. Brady and P. G. Pentchev. 1992. Progesterone blocks cholesterol translocation from lysosomes. *J. Biol. Chem.* **267**.
45. Gu, J., X. Y. Guan, and M. A. Ashlock. 1999. Isolation of human transcripts expressed in hamster cells from YACs by cDNA representational difference analysis. [In Process Citation] *Genome Res.* **9:** 182–188.
46. Jiang, L. W., V. M. Maher, J. J. McCormick, and M. Schindler. 1990. Alkalinization of the lysosomes is correlated with ras transformation of murine and human fibroblasts. *J. Biol. Chem.* **265:** 4775–4777.
47. Martinez- Botas, J., A. J. Ferruelo, Y. Suarez, C. Fernandez, D. Gomez-Coronado, and M. A. Lasuncion. 2001. Dose-dependent effects of lovastatin on cell cycle progression. Distinct requirment of cholesterol and non-sterol mevalonate derivatives. *Biochim. Biophys. Acta.* **1532:** 185–194.
48. Jordens, I., M. Fernandez-Borja, M. Marsman, S. Dusseljee, L. Janssen, J. Calafat, H. Janssen, R. Wubbolts, and J. Neefjes. 2001. The Rab7 effector protein RILP controls lysosomal transport by inducing the recruitment of dynein-dynactin motors. *Curr. Biol.* **11:** 1680–1685.
49. Choudhury, A., M. Dominguez, V. Puri, D. K. Sharma, K. Narita, C. L. Wheatley, D. L. Marks, and R. E. Pagano. 2002. Rab proteins mediate Golgi transport of caveola-internalized glycosphingolipids and correct lipid trafficking in Niemann-Pick C cells. *J. Clin. Invest.* **109:** 1541–1550.
50. Mu, J., and L. X. Wei. 2002. Telomere and telomerase in oncology. *Cell Res.* **12:** 1–7.